Organic/Inorganic-Polyimide Nanohybrid Materials for Advanced Opto-Electronic Applications

Shinji Ando*
Department of Chemistry & Materials Science, Tokyo Institute of Technology,
Ookayama 2-12-1, Meguro-ku, Tokyo 152-8552, JAPAN

ABSTRACT

Nano-hybridization techniques based on the pyrolytic reactions of organo-soluble metallic precursors dissolved in poly(amic acid)s followed by spontaneous precipitation of metal/inorganic nano-particles in solid polyimide (PI) films is facile and effective for functionalization of PI optical and electronic materials. The organic/inorganinc PI nanohybrid materials, which were recently developed by the authors, having a variety of functionalities such as a) high refractive indices, b) low refractive indices, c) controlled thermo-optical property and its anisotropy, d) high polarizing property, and e) high thermal conductivity are reviewed with future prospects on their advanced opto-electronic applications.

Keywords: Nanohybrid, nano-particles, polyimide, refractive index, birefringence, thermo-optic coefficient, polarizer, thermal conductivity, phase separation, double percolation

1. INTRODUCTION

The advantages of polymers in the application to optical components, such as micro-lens for CCD/CMOS image sensors, thin films and anti-reflective coatings for flat-panel displays (LCD and OLED), and waveguide circuits in optical interconnects and telecommunications, are 1) facile formation of thin films at lower temperatures, 2) light-weight, toughness, and flexibility, 3) micro-patternability by phtolithography or imprinting, 4) wide range of molecular design, and 5) facile incorporation of metallic or inorganic dopants or nano-particles.[1-5] In contrast, the drawbacks of polymeric materials are a) low thermal stability, b) high moisture absorption, c) low environmental stability and durability, d) narrow range of controllable optical properties such as transmittance, wavelength range with high transparency, refractive indices, birefringence, and thermo-optic coefficients, and e) low thermal conductivity. Recently, with the rapid development of nano-science and nanotechnology, various methods to provide functional optical polymers have been revealed. In particular, nano-hybridization of polymers with metallic or inorganic nano-particles is a promising technique to overcome the drawbacks without reducing their inherent advantages.[6-9] When the sizes of nano-particles are smaller than 40 nm (~1/10 of the visible wavelengths), nanohybrid films are generally transparent. The sol-gel method is a wet-chemical process for the fabrication of metal oxide starting from a organic solution undergoing hydrolysis and polycondensation reactions followed by drying and thermal curing for further condensation and consolidation, and it is a promising technology. Since the sol-gel process uses organo-soluble compounds as source materials, it can afford metal oxide such as SiO_2, ZrO_2, ZnO, TiO_2, Al_2O_3 at much lower temperatures than thermal fusion method. Furthermore, polyimides (PIs) are generally cured at higher temperatures (250~400°C) than conventional optical polymers, which enables to use wider range of precursors as source materials for metallic and inorganic nano-particles.[10-14]

2. HIGH REFRACTIVE POLYIMIDES

High refractive index (high-n) and low birefringence (Δn) combined with good thermal stability and high transparency are the basic concerns in designing polymer coatings for micro-lens applications. According to the Lorentz-Lorenz equation (1), the wavelength (λ)-dependent refractive index (n_λ) of a solid polymer can be expressed as

$$\frac{n_\lambda^2 - 1}{n_\lambda^2 + 2} = \frac{4\pi}{3} K_p \frac{\alpha_\lambda}{V_{vdw}}, \quad (1)$$

Organic Photonic Materials and Devices XI, edited by Robert L. Nelson, François Kajzar, Toshikuni Kaino
Proc. of SPIE Vol. 7213, 72130B · © 2009 SPIE · CCC code: 0277-786X/09/$18 · doi: 10.1117/12.814976

where K_p is the molecular packing coefficient, α_λ the wavelength-dependent molecular polarizability of a repeating unit, and V_{vdw} the van der Waals volume of a repeating unit. The wavelength dispersion of refractive indices in the visible region is usually estimated by Abbe number (ν) which is defined as equation (2).

$$\nu = \frac{n_{589} - 1}{n_{486} - n_{656}} \tag{2}$$

Transparent and colorless polyimides[15] with high refractive indices and high Abbe numbers are preferable for thermally stable lens applications. We have demonstrated that the density functional theory (DFT) calculations using the B3LYP hybrid functional can reproduce the wavelength-dependent refractive indices of eight-six organic compounds with high accuracy.[16-19] As shown in Fig. 1, the experimental Abbe numbers (ν_{exp}) are well reproduced by the calculated values (ν_{cal}) with the square correlation factor (r^2) of 0.978 as accompanied by the good correlation between the experimental (n_{exp}) and calculated refractive indices (n_{cal}).[19] These relations clearly indicate that the DFT is a useful tool to predict the optical properties of novel polymers suitable to specific applications.

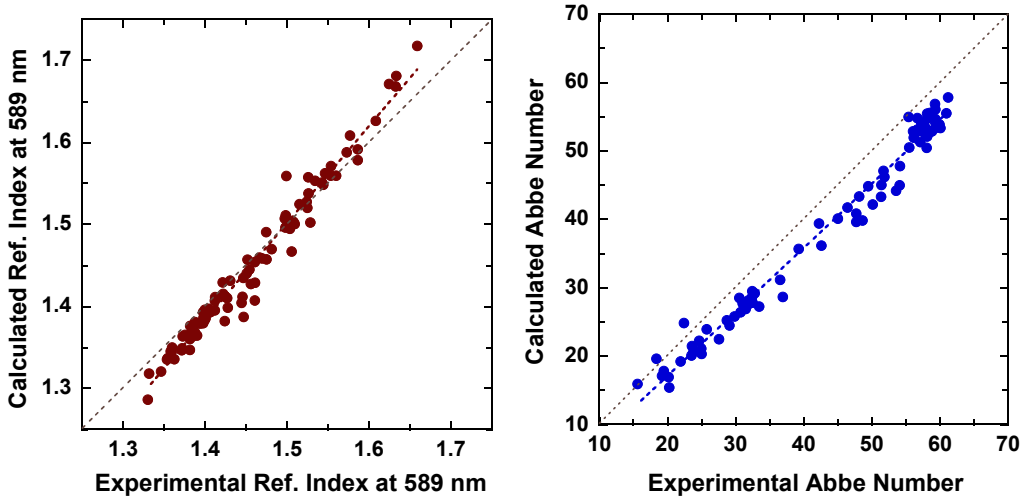

Fig. 1 Relationships between the experimental and calculated (a) refractive indices and (b) Abbe numbers for eighty-six organic compounds. The refractive indices are the values at 589 nm.

Conventional polymers could be endowed with high refractive indices by introducing substituents having higher molar refraction and lower free molecular volumes. In particular, sulfur-containing substituents are one of the most promising candidates. Terui et al. have reported that a PI derived from 3,3',4,4'-biphenyltetracarboxylic dianhydride (sBPDA) and bis(4-aminophenyl)disulfide exhibit a very high n of 1.698 with a low birefringence of 0.09.[20] Scheme 1 shows the sulfur-containing PIs designed and synthesized by Liu, Ando, Ueda et al.[21-31] The optical absorption spectra and the refractive index dispersions of the PIs derived from APTT diamine and s-BPDA dianhydride are shown in Figs. 2 and 3. The PI (3SDEA-APTT) with the highest sulfur content of 23.2 % shows the highest n of 1.761 at 632.8 nm. This is one of the highest values in high-n polymers.

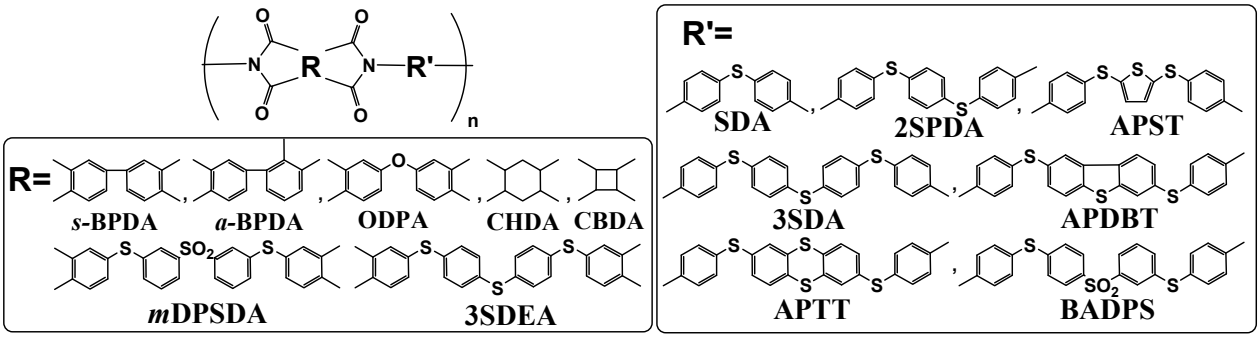

Scheme 1 Sulfur-containing fully- and semi-aromatic polyimides (PIs) exhibiting high refractive indices.

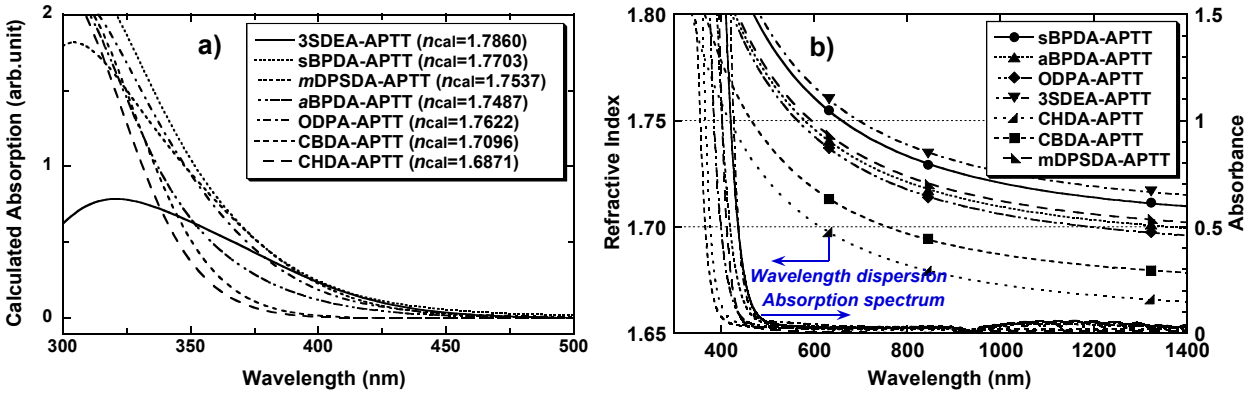

Fig. 2 a) Calculated absorption spectra with calculated refractive indices (inset), and b) experimental absorption spectra and wavelengths dispersion of refractive indices of the PI films derived from APTT diamine.

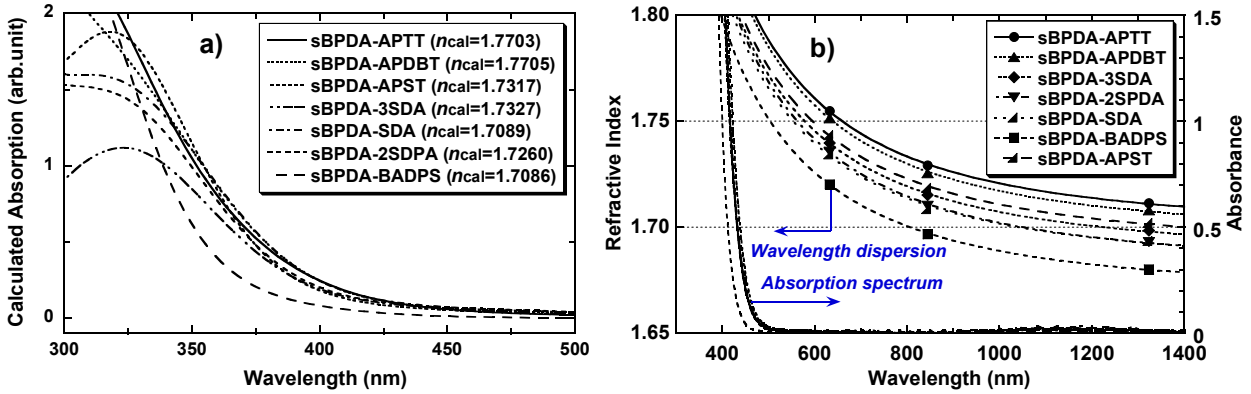

Fig. 3 a) Calculated absorption spectra with calculated refractive indices (inset), and b) experimental absorption spectra and wavelengths dispersion of refractive indices of the PI films derived from sBPDA dianhydride.

As shown Figs 2 and 3, the experimental absorption edges agree well with the calculated values obtained by TD-DFT method, and the refractive index dispersions are well fitted by the simplified Cauchy's formula ($n_\lambda = n_\infty + D/\lambda^2$).[33] The n_∞ reflects the inherent refractive index of a PI, which is not influenced by the electronic absorptions in the UV region. Figure 4 shows the relationships between the values of n_∞ and D, which were obtained from thirty kinds of PIs. Two different linear relationships are observed for the semi-alicyclic and aromatic PIs, respectively, which agree well with the relation that we have reported previously.[33] The higher n, the larger D, which straightforwardly indicates that a high-n rarely exists with a low D. Among the various dianhydrides, ODPA and *m*DPSDA dianhyrides having lower electron affinities, can provide PIs with higher transparency and lower dispersion.

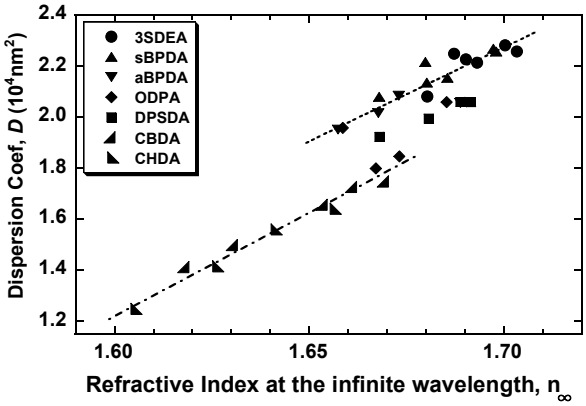

Fig. 4 Relations between the n_∞ values and the dispersion coefficients (D) for the PIs derived from various dianhydrides.

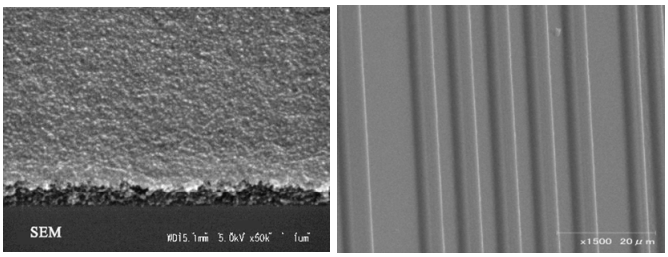

Fig.5 SEM pictures of PI(CHDA-APTT)−TiO2 (55:45 w/w) nanochybrid film and 4 μm-pitch negative patterns (1 μm-thick).

PI (CHDA-APTT) exhibits the highest optical transparency with n=1.680 and Δn=0.0048. Thus, it was combined with SiO_2-modified TiO_2 nano-particles.[25] The poly(amic acid) (PAA) solution showed good affinity with nano-particles up to the proportion of poly(amic acid) (PAA):TiO_2=55:45 (w/w) (Fig. 5). The homogeneous and transparent PI thin film has a very high n of 1.810, which achieves the target for micro-lens for CCD (n >1.80).

3. LOW REFRACTIVE POLYIMIDES

Low refractive index (low-n) materials also have a high demand for anti-reflective coatings and OLED applications. We have been developing PIs exhibiting high transparency with low refractive indices by introducing fluorines and alicyclic structures in the main chain.[34,35] The PI (6FDA-DCHM) shows a low n of 1.509 with a low Δn of 0.001 at 1324 nm. We attempted to lower the n of PI by incorporating magnesium fluoride (MgF_2) nano-particles. MgF_2 is known as a representative low-n inorganic glass with a refractive index of 1.38 at 633 nm. Since $Mg(CF_3COO)_2 \cdot nH_2O$ (MgTfAc) can be thermally converted to MgF_2 under nitrogen at ca. 300°C recently,[36] MgTfAc was dissolved in a DMAc solution of PAA of 6FDA-DCHM to afford a precursor for PI containing MgF_2 nanoparticles.

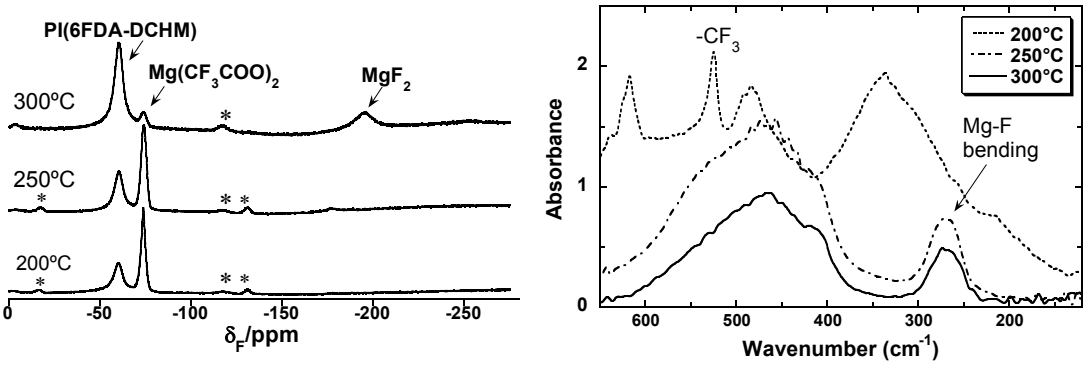

Fig. 6 Solid state ^{19}F MAS (left) and b) FT-FarIR spectra (right) of PI (6FDA-DCHM) films hybridized with MgTfAc (100 mol%) cured in vacuo at 200, 250, and 300°C.

Figure 6 shows the ^{19}F magic-angle spinning (MAS) NMR and Fourier-transformed (FT) far-infrared (Far-IR) absorption spectra of the hybrid films thus obtained, which demonstrate that 93.3% of MgTfAc was converted to MgF_2 by curing at 300°C, whereas MgTfAc was unchanged at 200 and 250°C despite the complete imidization of PAA at 200°C. The hybrid films cured at 200 and 250°C are perfectly colorless and transparent, which is same as the pristine PI film. Since amorphous MgF_2 crystallizes over 600°C,[36] no diffraction peaks characteristic to MgF_2 were observed in the WAXD patterns of all films. Figure 7 shows the curing temperature dependence of the refractive indices of the PI nanohybrid films prepared with different MgTfAc contents. The observed n values were systematically reduced by −2.15, −2.04, −0.83 % by the incorporation of MgTfAc (150 mol%) to the PIs cured at 200, 250 and 300°C, respectively. Note that the n values of the films cured at 200 and 250°C are significantly lower than those at 300°C. MgTfAc was unchanged in the former but decomposed to MgF_2 in the latter, which indicates that the inherent refractive index of MgTfAc is significantly lower than that of MgF_2 due to the lower density and higher fluorine content. The n value of 1.477 at 1324 nm is one of the lowest values in low-n polymers, and its high thermal stability is a great advantage.

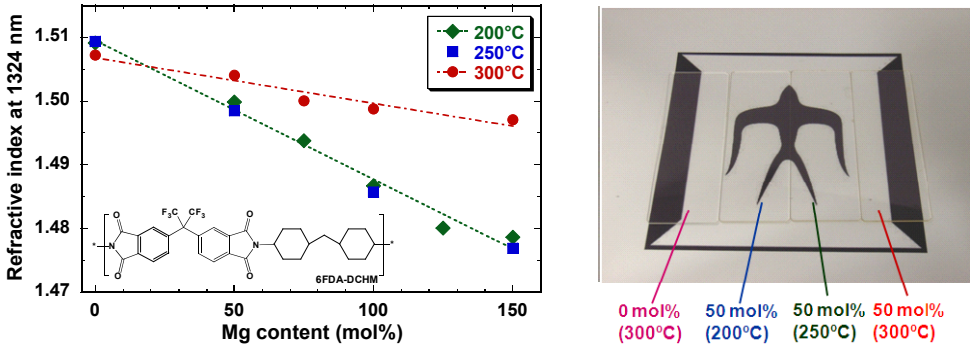

Fig. 7 Refractive indices of PI (6FDA-DCHM) films hybridized with different amounts of MgTfA cured at 200, 250, and 300°C, respectively (left), and the photos of PIs formed on glass substrates (right).

4. POLYIMIDE THIN FILMS WITH CONTROLLED THERMO-OPTIC COEFFICIENTS

The temperature dependence of refractive indices ($|dn/dT|$) of polymers, which is called 'thermo-optic coefficients', is significantly larger than those of inorganic glasses because polymers possess much larger thermal expansion. Hence, optical polymers are suitable for the materials for thermo-optical switches and wavelength-selective arrayed waveguide (AWG) filters. In order to achieve a larger $|dn/dT|$, a higer refractive index and/or a larger thermal expansion are required. Introduction of sulfur atoms or aromatic rings are effective for the former, and an increase in free volume is significant for the latter.[37-40] As shown in Fig. 8, it was demonstrated that the introduction of siloxane linkages in the main chain of PIs effectively lower the glass transition temperature (T_g) to 60°C, and the values of $|dn/dT|$ can be increased to 350 ppm/K[40] (typical values below T_g are ca. 70−100 ppm/K). In addition, the application of sol-gel process using tetraethoxysilane (TEOS) as a silica (SiO_2) source successfully endows good solvent resistivity to the PIs. The introduction of SiO_2 by 10 wt% significantly raises the T_g, which simultaneously enables to control the values of $|dn/dT|$.

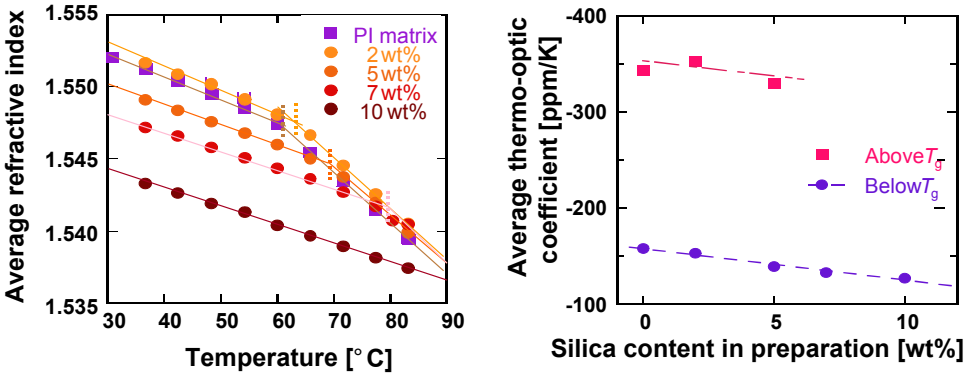

Fig. 8 Temperature dependence of n_{av} of PI/silica nanohybrid films (left), and the silica-content dependence of dn_{av}/dT for the PI hybrid films below and above T_g (right).

Although PI/silica nanohybrids seems to exhibit smaller $|dn/dT|$ due to the formation of silica networks, an apparent increase in $|dn/dT|$ was observed at lower SiO_2 contents, and then turned to decrease at higher SiO_2 contents. A similar tendency was observed for the polarization anisotropy in $|dn/dT|$, which corresponds to the temperature dependence of in-plane/out-of-plane birefringence (Δn). We have clarified that these parameters are proportional to the thermal expansion coefficients along the out-of-plane direction ($\alpha_\perp$)[41] (Fig. 9). These facts indicates that, at lower silica contents, volume thermal expansion is instantly increased due to the increase in free volumes between PI chains and nano-particles. Since PI films are formed on silicon substrates, in-plane thermal expansion is suppressed, and vertical (out-of-plane) expansion is enhanced, which is the reason of the simultaneous increases in $\alpha_\perp$, $|dn/dT|$, and $|d(\Delta n)/dT|$. In contrast, at higher silica contents, the thermal volume expansion is effectively suppressed by the growing silica networks which effectively reduce the $|dn/dT|$, and $|d(\Delta n)/dT|$.

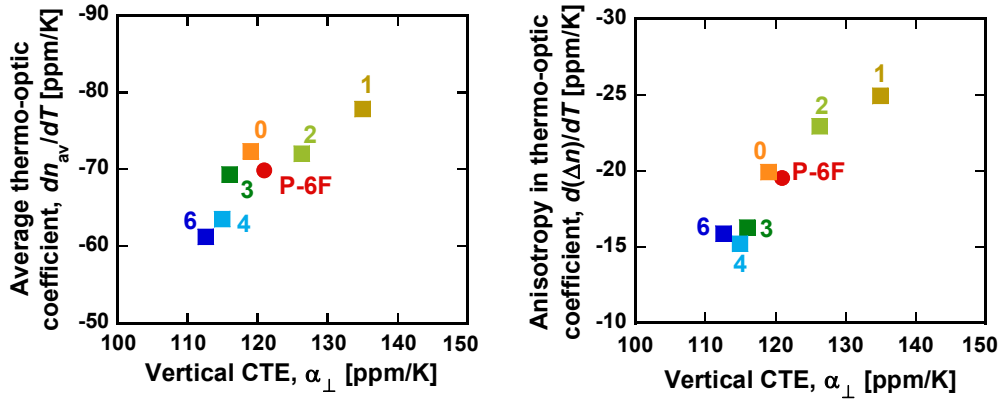

Fig. 9 Relationships between the thermal expansion coefficients along the out-of-plane direction (vertical CTE, $\alpha_\perp$) and dn/dT (left) and $d(\Delta n)/dT$ (right) for silica-PI nanohybrid films. P-6F corresponds to the pristine PI (6FDA-TFDB), and the numbers attached to data-points denote the silica contents (wt%) in preparation.

5. POLYIMIDE THIN FILM POLARIZER

Linear polarizing films made of poly(vinyl alcohol) films dyed with iodine (I_2) are widely used for liquid crystalline displays (LCDs), but this type of films cannot be used for optical communication applications because iodine does not exhibit anisotropic absorptions in the near-infrared (NIR) region. Instead, inorganic polarizer fabricated by uniaxial elongation of silver or copper nano-particles dispersed in inorganic glasses are used in fiber-optic devises such as optical isolators. Metal nano-rods show significant polarizing properties in the visible-NIR regions, though glass matrix have drawbacks in the thickness (150~200 μm), fragility, processability, and mass-production. Hence, we tried to fabricate thin film polarizers based on silver nano-particles dispersed in colorless and transparent PIs having rigid-rod structures.[42-45] As shown in Fig. 10, a new series of copolymers consisting of a sulfur-containing PAA having high affinity to noble metals and a fluorinated PAA having low affinity were prepared, and silver nitrate was dissolved in a DMAc solution of the PAA. Due to the large difference in hydrophobicity between the two components, the dried PAA films exhibited typical micro-phase separation, and energy dispersive spectroscopy (EDS) clarified that nanometer-sized silver particles were selectively concentrated and precipitated in the sulfur-rich domain. During simultaneous curing and uniaxial drawing at higher temperatures (>350°C), the PI films showed apparent polarizing properties in the visible-NIR regions due to the deformed shapes of silver nano-particles. Since it has been reported that the melting temperatures (T_m) of metal nano-particles are significantly lower than those of bulk (T_m of bulk silver is 689°C), such nano-particles can be elongated at appropriate conditions (temperature, atmosphere, and tensile stress). We developed a new apparatus for the in-situ and real-time observation of polarized transmission spectra to monitor and control the temperature and drawing conditions. The silver nano-rods thus precipitated in the PI blend film show significantly elongated shapes (50−300 nm) with perfect orientation along the drawing direction (Fig. 10). The WAXD pattern of the film shows that these particles are nano-crystallites of zero-valent silver, and the PI film thus obtained shows very good polarizing property (dichroic ratio: >300 at 1550 nm) with high optical transmission (>70 %) as shown in Fig. 11. In addition, the PI film is only 15 μm-thick (ca. ~1/10 of inorganic polarizers), tough, and flexible, which leads to great advantages in processability and mass-production required for the applications in micro-optics and waveguide devises such as optical isolator.

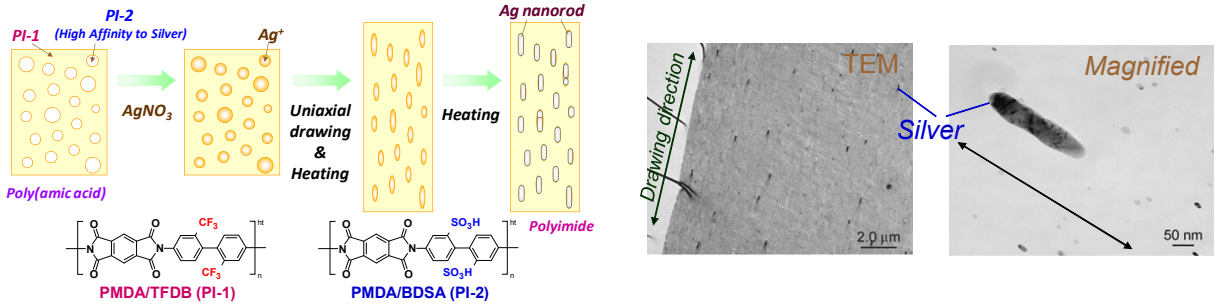

Fig. 10 Schematic representation of spontaneous condensation and precipitation of silver nano-particles having elongated shapes in the sulfur-containing phase in PI blend films (left) and TEM micrographs of the PI film with silver (right).

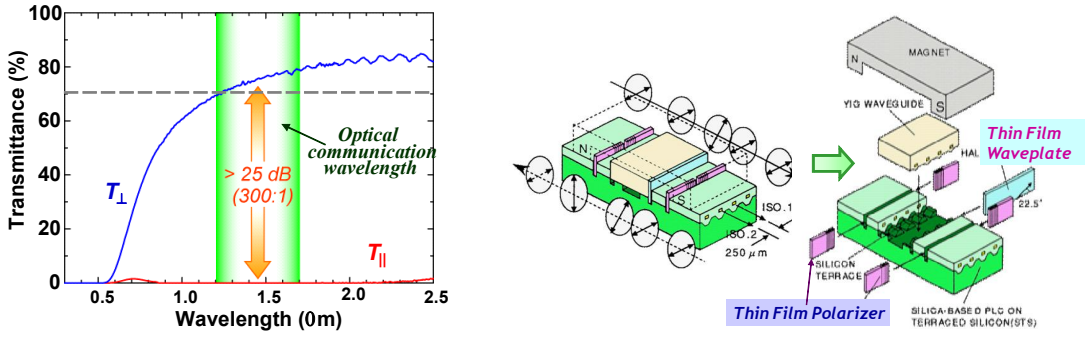

Fig. 11 Polarized optical transmission spectra of a PI film containing silver nanoparticles having elongated shapes, and an example of applications of PI thin film polarizer and half-waveplates for a waveguide-type optical isolator.

6. POLYIMIDE THIN FILMS WITH HIGH THEMAL CONDUCTIVITY

Thermally stable polymers with high thermal conductivity are strongly needed for efficient heat transfer in electronic applications. Polymers hybridized with metal oxide particles have been widely studied, but their improvement in thermal conductivity is limited due to the large interfacial thermal resistance between polymer and fillers. We have proposed a new strategic design for effective increase in thermal conductivity based on the selective precipitation of silver nano-particles in micro phase-separated PI blends as illustrated in Fig. 12.[46] PI blend films (sBPDA/SDA-TFDB) consisting of two-types of PIs having different affinities to silver ions were prepared. Silver nitrate ($AgNO_3$) dissolved in PAA solutions was thermally reduced to metallic silver during imidization, which forms silver nano-particles in the films. Fig. 12 shows the FE-SEM micrographs of the hybrid films, in which 'double percolation' structures orienting along the out-of-plane direction were clearly formed, and the average size of each phase is in ~10 μm order. Energy-dispersive X-ray spectroscopy (EDS) also showed that silver nano-particles were preferentially precipitated in the S-PI phase due to the high affinity with noble metals. The thermal diffusivity along the out-of-plane direction ($a_{\perp}$) were measured with an AC temperature-wave analyzer (thermal conductivity is the product of a and a specific heat). At 20 mol% of $AgNO_3$, the PI blend films of SDA:TFDB=50:50 (mol%) exhibit a higher thermal diffusivity than the pristine PI having homogeneously dispersed silver nanoparticles and the other PI blends having typical sea-island structures. This clearly implies that the double percolation structures thus generated function as thermal conductivity pathways along the out-of-plane direction.

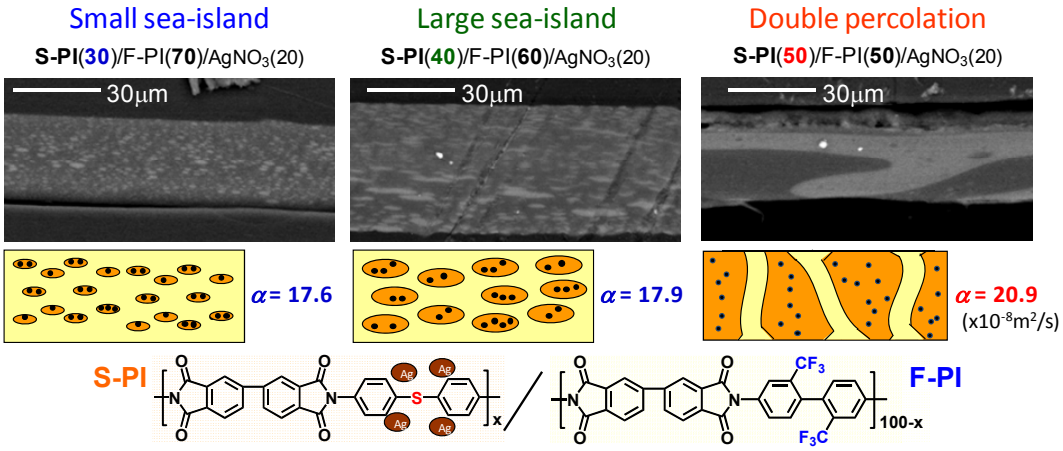

Fig. 12 Cross-sectional FE-SEM photographs of the micro phase-separated PI hybrid films consisting of sulfur-containing PI (S-PI) and fluorine-containing PI (F-PI). The phase separation and silver precipitation are schematically illustrated below the photos. The S-PI phase containing silver nano-particles are seen as white parts.

7. SUMMARY

Organic/inorganinc PI nanohybrid materials having optical functionalities, such a) high refractive indices (n=1.81), b) low refractive indices (n=1.47), c) controlled thermo-optical property ($|dn/dT|$ >350 ppm/K) and its anisotropy, d) high polarizing property (dichroic ratio > 25 dB), and e) good thermal conductivity have been developed by the nano-hybridization techniques based on the pyrolytic reactions (reduction, oxidation, and decomposition) of organo-soluble metallic precursors followed by spontaneous precipitation of metal/inorganic nano-particles in solid PI films. This technique enables us to develop novel opt0-electronic materials having a variety of functionality with maintaining the inherent excellent properties of PIs.

Acknowledgement : The author acknowledges that the results reviewed in this paper have been obtained by fruitful collaborations with Prof. Mitsuru Ueda, Yuji Shibasaki, Sho-ichi Matsuda, Yoshiharu Terui, Akiko Matsumura, Yasuo Suzuki, Nam Ho You, Atsuhisa Suzuki, Yasuhiro Nakamura (Tokyo Tech), Jin-gang Liu (present: the Chinese academy of science), and Claudio A. Terraza (present: Pontificia univ. Catolica de Chile).

REFERENCES

[1] Sullivan, C. T., Proc. SPIE, 994, 92 (1988).
[2] Reuter, R., Franke, H. and Feger, C., Applied Optics, 27, 4565 (1988).
[3] Franke, H., Wagner, D., Kleckers, T., Reuter, R., Rohitkumar, H.V. and Blech, B.A., Applied Optics, 32, 2927 (1993).
[4] Hougham, G., Cassidy, P.E., Johns, K. and Davidson, T., eds. "Fluoropolymers 1: Synthesis and 2: Properties", Kluwer Academic/ Plenum Publishers, New York (1999).
[5] Ando, S., J. Photopolym. Sci. Technol., 17, 219 (2004).
[6] Weibel, M., Caseri, W., Suter, U.W., Kiess, H. and Wehrli, E., Adv. Mater., 2, 75 (1991).
[7] Zimmermann, L., Weibel, M., Caseri, W.U., Suter, W. and Walther, P., Polym. Adv. Technol., 4, 1 (1993).
[8] Althues, H., Henle, J. and Kaskel, S., Chem. Soc. Rev., 36, 1454 (2007).
[9] Kickelbick, G., 'Hybrid Materials, Synthesis, Characterization, and Applications', Wiley-VCH (2007).
[10] St. Clair, A.K. and Taylor, L.T., J. Appl. Polym. Sci., 28, 2393 (1983).
[11] Rancourt, J.D., Porta, G.M. and Taylor, L.T., Chem. Mater.,1, 269 (1989).
[12] Ellison, M.W. and Taylor, L.T., Chem. Mater., 6, 990 (1994).
[13] Rubira, A.F., Rancourt, J.D., Caplan, M.L., St.Clair, A.K. and Taylor, L.T., Chem. Mater., 6, 2351 (1994).
[14] Sawada T. and Ando, S., Chem. Mater., 10, 3368 (1998).
[15] Ando, S., Matuura, T. and Sasaki, S., Polymer J., 29, 69 (1997).
[16] Ando, S., Fujigaya, T. and Ueda, M., Jpn. J. Appl. Phys., 41, L105 (2002).
[17] Ando, S., Fujigaya, T. and Ueda, M., J. Photopolym. Sci. Technol., 15, 559 (2002).
[18] Ando, S. and Ueda, M., J. Photopolym. Sci. Technol., 16, 537 (2003).
[19] Ando, S. J. Photopolym. Sci. Technol., 19, 351 (2006).
[20] Terui, Y. and Ando, S., J. Photopolym. Sci. Technol., 18, 337 (2005).
[21] Liu, J.-G., Nakamura, Y., Shibasaki, Y., Ando, S. and Ueda, M., Polym. J., 39, 543 (2007).
[22] Liu, J.-G., Nakamura, Y., Shibasaki, Y., Ando, S., Ueda, M., Macromolecules, 40, 4614 (2007).
[23] Liu, J.-G., Nakamura, Suzuki, Y., Y., Shibasaki, Y., Ando, S. and Ueda, M., Macromolecules, 40, 7902 (2007).
[24] Liu, J.-G., Nakamura, Y., Suzuki, Y., Shibasaki, Y., Ando, S. and Ueda, M., J. Polym. Sci. Part A, Polym Chem., 45, 5606 (2007).
[25] Liu, J.-G., Nakamura, Y., Ogura, T., Shibasaki, Y., Ando, S. and Ueda, M., Chem. Mater., 20, 273 (2008).
[26] Liu, J.-G., Shibasaki, Y., Ando, S. and Ueda, M., High Perform. Polym., 20, 221 (2008).
[27] Liu, J.-G., Nakamura, Y., Terraza, C.A., Shibasaki, Y., Ando, S. and Ueda, M., Macromol. Chem. Phys., 209, 195 (2008).
[28] C.A. Terraza, Liu, J.-G., Nakamura, Y., Shibasaki, Y., Ando, S. and Ueda, M., J. Polym. Sci., Part A: Polym. Chem., 46, 1510 (2008).
[29] Suzuki, Y., Liu, J.-G., Nakamura, Y., Shibasaki, Y., Ando, S. and Ueda, M., Polymer J., 40, 414
[30] You, N.-H., Suzuki, Y., Yorifuji, D., Ando, S. and Ueda, M., Macromolecules, 41, 6361 (2008).
[31] You, N.-H., Suzuki, Y., Higashihara, T., Ando, S. and Ueda, M., Polymer (2009) (*in press*).
[32] Suzuki, Y., Nakamura, Y., Ando, S. and Ueda, M., J. Photopoly. Sci. Technol., 21, 131 (2008).
[33] Ando, S., Watanabe, Y. and Matsuura, T., Jpn. J. Appl. Phys. Part 1, 41, 5254 (2002).
[34] Ando, S., Suzuki, A., Nakamura, Y., Liu, J.-G. and Ueda, M., Proc. STEPI, 8, (2008) (*in press*).
[35] Matsuda, S., Urano, Y., Park, J.-W., Ha, C.-S. and Ando, S., J. Photopolym. Sci. Technol., 17, 241 (2004).
[36] Fujihara, S., Tada, M. and Kimura, T., Thin Solid Films, 304, 252 (1997), *ibid*, 389, 227 (2001).
[37] Terui, Y. and Ando, S., Appl. Phys. Lett., 83, 4755 (2003).
[38] Terui, Y. and Ando, S., J. Photopolym. Sci. Technol., 18, 337 (2005).
[39] Terui, Y. and Ando, S., Proc. SPIE, 5724, 336 (2005).
[40] Terui, Y. and Ando, S., High Perform. Polym., 18, 825 (2006).
[41] Matsumura, A., Terui, Y., Ando, S., Abe, A. and Takeichi, T., J. Photopolym. Sci. Technol., 20, 167 (2007).
[42] Sawada, T., Ando, S. and Sasaki, S., Appl. Phys. Lett., 74, 938 (1999).
[43] Matsuda, S., Ando, S. and Sawada, T., Electron. Lett., 37, 706 (2001).
[44] Matsuda, S. and Ando, S., Polym. Adv. Technol., 14, 458 (2003).
[45] Matsuda, S., Yasuda, Y. and Ando, S., Adv. Mater., 17, 2221 (2005).
[46] Yorifuji, D. and Ando, S., (submitted for publication).